

Regression of apoptosis-resistant colorectal tumors by induction of necroptosis in mice

Gui-Wei He,¹ Claudia Günther,¹ Veronika Thonn,¹ Yu-Qiang Yu,¹ Eva Martini,¹ Barbara Buchen,¹ Markus F. Neurath,¹ Michael Stürzl,² and Christoph Becker¹

¹Department of Medicine 1 and ²Division of Molecular and Experimental Surgery, Department of Surgery, University of Erlangen-Nuremberg, 91054 Erlangen, Germany

Cancer cells often acquire capabilities to evade cell death induced by current chemotherapeutic treatment approaches. Caspase-8, a central initiator of death receptor-mediated apoptosis, for example, is frequently inactivated in human cancers via multiple mechanisms such as mutation. Here, we show an approach to overcome cell death resistance in *caspase-8*-deficient colorectal cancer (CRC) by induction of necroptosis. In both a hereditary and a xenograft mouse model of *caspase-8*-deficient CRC, second mitochondria-derived activator of caspase (SMAC) mimetic treatment induced massive cell death and led to regression of tumors. We further demonstrate that receptor-interacting protein kinase 3 (RIP3), which is highly expressed in mouse models of CRC and in a subset of human CRC cell lines, is the deciding factor of cancer cell susceptibility to SMAC mimetic-induced necroptosis. Thus, our data implicate that it may be worthwhile to selectively evaluate the efficacy of SMAC mimetic treatment in CRC patients with *caspase-8* deficiency in clinical trials for the development of more effective personalized therapy.

INTRODUCTION

Caspase-8 plays a central role in initiating apoptosis upon activation of death receptors by extrinsic factors such as TNF (Degterev et al., 2003). Recent studies have indicated that caspase-8 is frequently inactivated in human cancers via multiple mechanisms, including gene mutations, epigenetic modifications, and posttranslational changes (Fulda, 2009). The inactivation of caspase-8 in cancer cells can cause evasion of apoptosis, a hallmark of cancer that also represents a key mechanism of resistance to current cancer treatments (Hanahan and Weinberg, 2011). In line with this, mutated *caspase-8* has been detected in human colorectal cancers (CRCs) and demonstrated to interfere with the recruitment of WT caspase-8 to activated death receptors in a dominant-negative fashion (Kim et al., 2003; Li et al., 2014). Importantly, a recent study has reported that *caspase-8* mutations are found in ~30% of hypermutated human CRCs (Cancer Genome Atlas Network, 2012). Until now, apoptosis resistance has remained a major clinical challenge for cancer treatment.

Recent studies of cell death research have uncovered a novel function of caspase-8 in inhibiting receptor-interacting protein kinase 3 (RIP3)-dependent necroptosis (Vandenaabee et al., 2010). The inactivation of caspase-8 (for example by mutations, silencing, or pharmacological inhibition) is protective against apoptosis and renders cells highly susceptible to RIP3-mediated necroptotic cell death (He et al., 2009;

Günther et al., 2011; Kaiser et al., 2011; Oberst et al., 2011), highlighting the potential to induce tumor cell necroptosis in apoptosis-resistant cancer patients.

Second mitochondria-derived activator of caspase (SMAC) mimetics, a class of drugs that mimics the endogenous activity of SMACs, have proven safe in phase 1 clinical trials in cancer patients (Fulda and Vucic, 2012). By promoting ubiquitination of cellular inhibitor of apoptosis (cIAP) proteins, such as cIAP1 (Birc2) and cIAP2 (Birc3), SMAC mimetics foster degradation of cIAPs to activate apoptosis (Fulda and Vucic, 2012). Because of its proapoptotic function, SMAC is implicated in a broad spectrum of tumors, and small-molecule SMAC mimetics have been developed to improve current cancer treatments (Petersen et al., 2007). Recent studies on necroptosis in cell lines have demonstrated that SMAC mimetics can also promote formation of the ripoptosome, a necroptotic signaling complex comprising caspase-8, FADD, RIP1, and RIP3, when the activity of caspase-8 is blocked (He et al., 2009; Feoktistova et al., 2011). SMAC mimetics thus might represent an attractive new strategy for overcoming apoptosis resistance specifically in *caspase-8*-deficient CRCs by inducing necroptosis.

RESULTS AND DISCUSSION

Our recent studies have demonstrated an essential survival function of caspase-8 in regulating intestinal homeostasis by inhibiting intestinal epithelial cell (IEC) necroptosis (Günther

Correspondence to Christoph Becker: christoph.becker@uk-erlangen.de

Abbreviations used: AOM, azoxymethane; CRC, colorectal cancer; DSS, dextran sodium sulfate; IEC, intestinal epithelial cell; NAS, necrosulfonamide; SMAC, second mitochondria-derived activator of caspase; TUNEL, terminal deoxynucleotidyl transferase dUTP nick end labeling; zVAD, Z-VAD-FMK.

© 2017 He et al. This article is distributed under the terms of an Attribution-Noncommercial-Share Alike license for the first six months after the publication date (see <http://www.rupress.org/terms/>). After six months it is available under a Creative Commons License (Attribution-Noncommercial-Share Alike 4.0 International license, as described at <https://creativecommons.org/licenses/by-nc-sa/4.0/>).



et al., 2011, 2015; Wittkopf et al., 2013). In line with these studies, we found that mice with an IEC-specific deletion of *caspase-8* (*Casp8 Δ IEC*) showed enhanced accumulation of RIP3 protein in IECs (Fig. 1, A and B). We next investigated whether increased levels of RIP3 in *caspase-8*-deficient IECs could affect their susceptibility to SMAC mimetic treatment. Strikingly, oral administration of 50 mg/kg of the SMAC mimetic LCL161, which had no obvious effect on the epithelial structure of the gut from WT mice, induced complete tissue destruction shown by staining with hematoxylin and eosin (H&E) and β -catenin, accompanied by massive cell death in both the small intestine and colon of *Casp8 Δ IEC* mice within only 24 h after treatment (Fig. 1 C and Fig. S1 A). The significant demise of the stem cell marker *Olfm4* in small intestine and *Lgr5* in both small intestine and colon 6 h after LCL161 treatment, a time point at which the surface of both small intestine and colon were still intact, suggests that SMAC mimetics cause a rapid loss of stem cells (Fig. S1, B and C). Furthermore, SMAC mimetic treatment, although safe for WT mice, led to 100% lethality in *Casp8 Δ IEC* mice within 4 d (Fig. 1 D). The lethal phenotype after SMAC mimetic treatment could be completely rescued by further depletion of either *Tnf receptor 1* (*Casp8 Δ IEC* \times *Tnfr1*^{-/-}) or *Rip3* (*Casp8 Δ IEC* \times *Rip3*^{-/-}; Fig. 1 D). On a tissue level, both *Casp8 Δ IEC* \times *Tnfr1*^{-/-} and *Casp8 Δ IEC* \times *Rip3*^{-/-} mice were resistant to SMAC mimetic-induced tissue destruction and epithelial cell death in the gut, which was comparable to WT mice (Fig. 1 E). Collectively, these data showed that IECs with *caspase-8* deficiency are hypersensitive to SMAC mimetic-induced necroptosis that required TNF receptor 1 signaling and RIP3.

To explore the implication of this finding for CRC treatment, we next sought to analyze the expression of necroptosis mediators in tumor cells. Intriguingly, in the *ApcMin/+* mouse model of CRC, the mRNA level of *Rip3* was approximately fourfold higher in tumors than in tumor-adjacent colon tissue, although no significant difference was observed in other necroptosis-related genes such as *Mkl1*, *Casp8*, *Birc1*, and *Birc2* (Fig. 2 A). In agreement with this finding, Western blotting showed a marked increment of RIP3 protein in *ApcMin/+* tumors compared with colon tissues (Fig. 2 B). Immunostaining further revealed that RIP3 was specifically up-regulated in tumor cells, but not in stromal cells (Fig. 2 C). Similar results were obtained when using a mouse model of colitis-associated cancer induced by a combination of azoxymethane (AOM)/dextran sodium sulfate (DSS; Fig. S1, D and E).

Given the increased levels of RIP3 in mouse tumor cells, we hypothesized that deficiency for *caspase-8*, such as it is observed in a group of CRC patients, could specifically sensitize tumors to SMAC mimetic-induced necroptosis. To test our hypothesis, we next crossed *ApcMin/+* mice with *Casp8 Δ IEC* mice to generate mice with *caspase-8*-deficient tumors (*ApcMin/+* \times *Casp8 Δ IEC*). Although histological analysis showed no significant differences in cell death when

comparing tumors from unchallenged *ApcMin/+* mice and *ApcMin/+* \times *Casp8 Δ IEC* mice, tumors with *caspase-8* deficiency showed elevated levels of RIP3 protein (Fig. 2, D and E; and Fig. S1 F). This finding was in agreement with previous studies indicating that *caspase-8* controls the cellular levels of RIP3 (Günther et al., 2011; Kaiser et al., 2011; Oberst et al., 2011). To avoid SMAC mimetic-induced epithelial destruction in the gut by systemic oral administration, we took advantage of interventional mouse colonoscopy and injected SMAC mimetics intratumorally (Becker et al., 2005; Neurath et al., 2010). Strikingly, local injection of LCL161 (100 μ g/tumor) led to significant tumor reduction in *ApcMin/+* \times *Casp8 Δ IEC* mice (from tumor size 4 to tumor size 1) in 6 d (Fig. 2, F and G). In contrast, the same dose of LCL161 did not reduce tumor size in *caspase-8*-proficient *ApcMin/+* mice (Fig. 2, F and G). Histological analysis of tumors collected 2 d after injection showed that LCL161 induced extensive tumor cell death and loss of β -catenin staining in *ApcMin/+* \times *Casp8 Δ IEC* mice, but not in *ApcMin/+* mice (Fig. 2 H). Collectively, these data showed that deficient *caspase-8* expression sensitizes mouse colon tumors to SMAC mimetic treatment.

Given that RIP3 plays a crucial role in necroptosis, we next asked whether RIP3 is a key factor of SMAC mimetic-induced necroptosis in human CRC cells. To address this question, we analyzed the expression of members of the necroptotic pathway in a panel of six human CRC cell lines (HT-29, HCT116, SW480, SW620, Caco2, and DLD-1). Compared with other necroptosis-regulating genes, including *MLKL*, *RIP1*, *CASP8*, and *FADD*, the mRNA levels of *RIP3* varied mostly among these cell lines (Fig. S2 A). In line with this, immunoblot further confirmed that RIP3 is also highly expressed on the protein level in HT-29 cells but weakly expressed in SW480 and SW620 cells and not detectable in HCT116, Caco2, and DLD-1 cells (Fig. S2 B). Intriguingly, the expression levels of RIP3 in these human cancer cells predicted susceptibility to SMAC mimetic-induced necroptosis in the presence of the caspase inhibitor Z-VAD-FMK (zVAD) in vitro (Fig. S2, C and D).

Given these findings, we next tested SMAC mimetic treatment in *caspase-8*-deficient human CRC cells. Using CRISPR-Cas9 technology, we generated a *caspase-8* knocked out HT-29 cell line (C8KO; Fig. 3 A). In contrast to control HT-29 cells, SMAC mimetic treatment induced a sharp decrease in the cell index as measured by xCELLigence real-time analysis (Fig. S2 E). Using propidium iodide staining, we found that within only 24 h, more than 80% of C8KO cells, but only few control cells, succumbed to SMAC mimetic treatment in vitro (Fig. 3 B). Strikingly, *caspase-8* deficiency reduced the half-maximal effective concentration of LCL161 in 48 h by 10,000-fold (Fig. S2 F). Using Western blotting, we observed increased levels of the RIP3 substrate MLKL phosphorylated at Ser358 in C8KO cells upon LCL161 stimulation, indicating that these cells might undergo necroptosis (Fig. 3 C). Indeed, preincubation with inhibitors of TNF (Enbrel), RIP1 (ne-

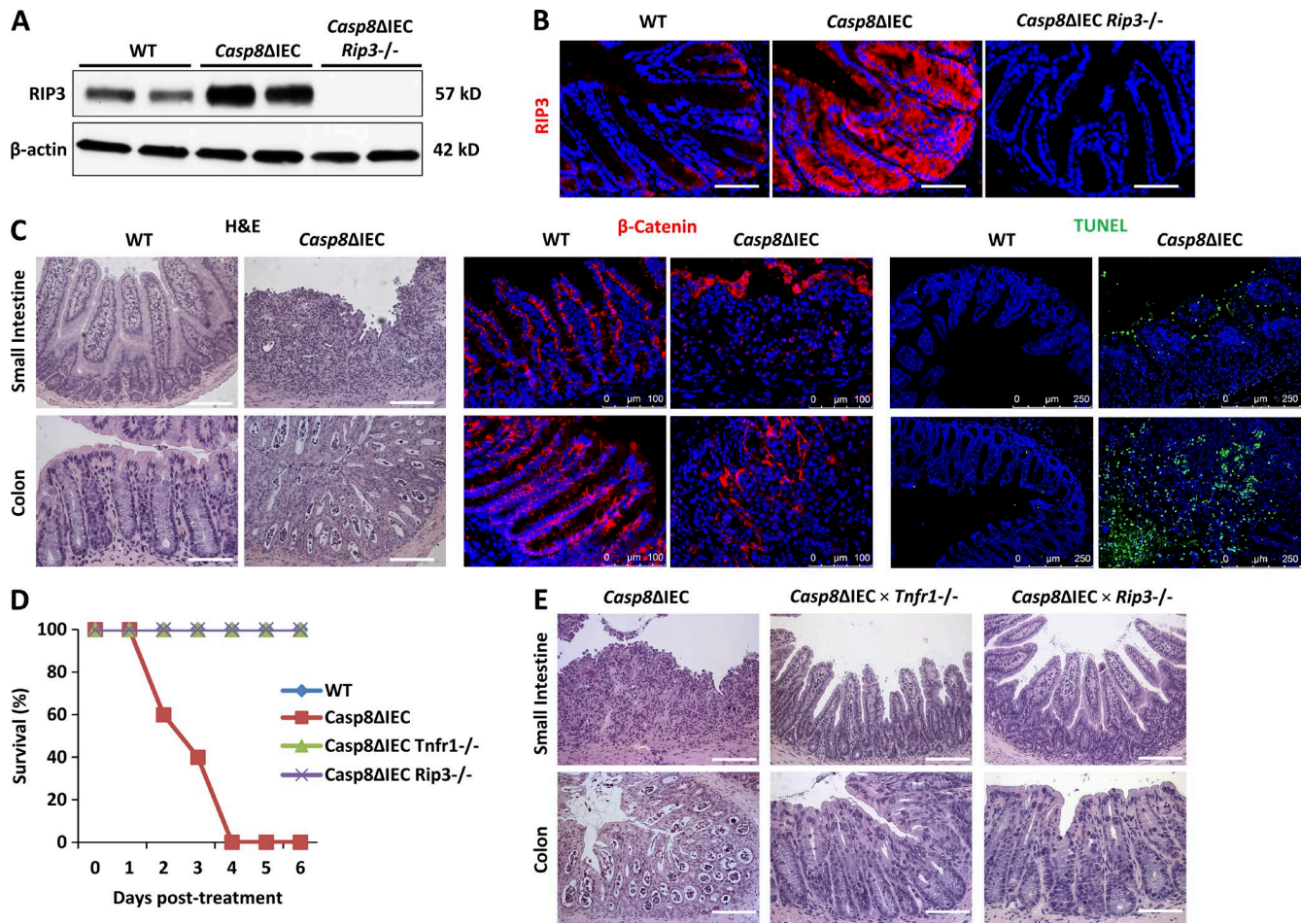


Figure 1. **Caspase-8-deficient IECs are hypersensitive to SMAC mimetic-induced necroptosis.** (A and B) RIP3 protein in colon tissues from the indicated mice was detected with immunoblots (β -actin served as a loading control; A) and immunostaining (B). Cell nuclei were counterstained with Hoechst 33342. Bars, 75 μ m. (C–E) WT, *Casp8* Δ IEC, *Casp8* Δ IEC \times *Tnfr1* $^{-/-}$, and *Casp8* Δ IEC \times *Rip3* $^{-/-}$ mice were treated with a single dose of 50 mg/kg LCL161 (oral). For histological analyses, tissues were collected 24 h after LCL161 administration. (C) Representative pictures of the small intestine and colon tissues from the indicated mice subjected to staining with H&E (left; bars, 75 μ m), β -catenin (middle), and TUNEL (right). Cell nuclei were counterstained with Hoechst 33342. (D) Kaplan–Meier survival curve. Group sizes: $n > 5$. (E) Representative pictures of small intestine and colon tissue from the indicated mice stained with H&E (left; bars, 75 μ m). Results from at least three biological replicates are presented unless otherwise specified. (D and E) Data derived from two independent animal experiments are shown.

crostain-1 [Nec-1]), or MLKL (necrosulfonamide [NAS]) completely protected C8KO cells from LCL161-induced cell death (Fig. 3 D and Fig. S2 G). Moreover, tumor cells with low, but not absent, caspase-8 expression generated by shRNA transfection were also significantly susceptible to SMAC mimetic-induced necroptosis in vivo (Fig. S3, F–H). Although TNF expression was elevated approximately eightfold in C8KO stimulated with LCL161 as compared with treated HT-29 control cells, neither C8KO cells treated with TNF nor HT-29 cells treated with TNF and LCL161 induced significant cell death (Fig. S2, H and I). This implies that *caspase-8* deficiency sensitized HT-29 cells to SMAC mimetic-induced necroptosis by cell-intrinsic mechanisms.

To ultimately demonstrate that SMAC mimetic alone is sufficient to induce regression of caspase-8-deficient human

colorectal tumors, we took advantage of an established xenograft model. Accordingly, we generated *caspase-8*-knockout HT-29 cells additionally carrying a luciferase expression cassette (HT-29-luc-D6) to track the cells in vivo. Cells were injected subcutaneously into *Rag1* $^{-/-}$ mice, and tumor development was monitored over time. Strikingly, oral administration of LCL161 resulted in rapid and substantial regression of C8KO-luc-D6 tumors measured by both a digital caliper and in vivo bioluminescent imaging, whereas *caspase-8*-proficient HT-29-luc-D6-derived tumors showed no significant difference in tumor development after treatment (Fig. 3, E and F). Accordingly, RT-PCR analysis of tumor tissues showed that the level of *TNFA* is elevated approximately eightfold in SMAC mimetic-treated C8KO tumors in comparison to treated HT-29 tumors and both untreated tumors (Fig. S3

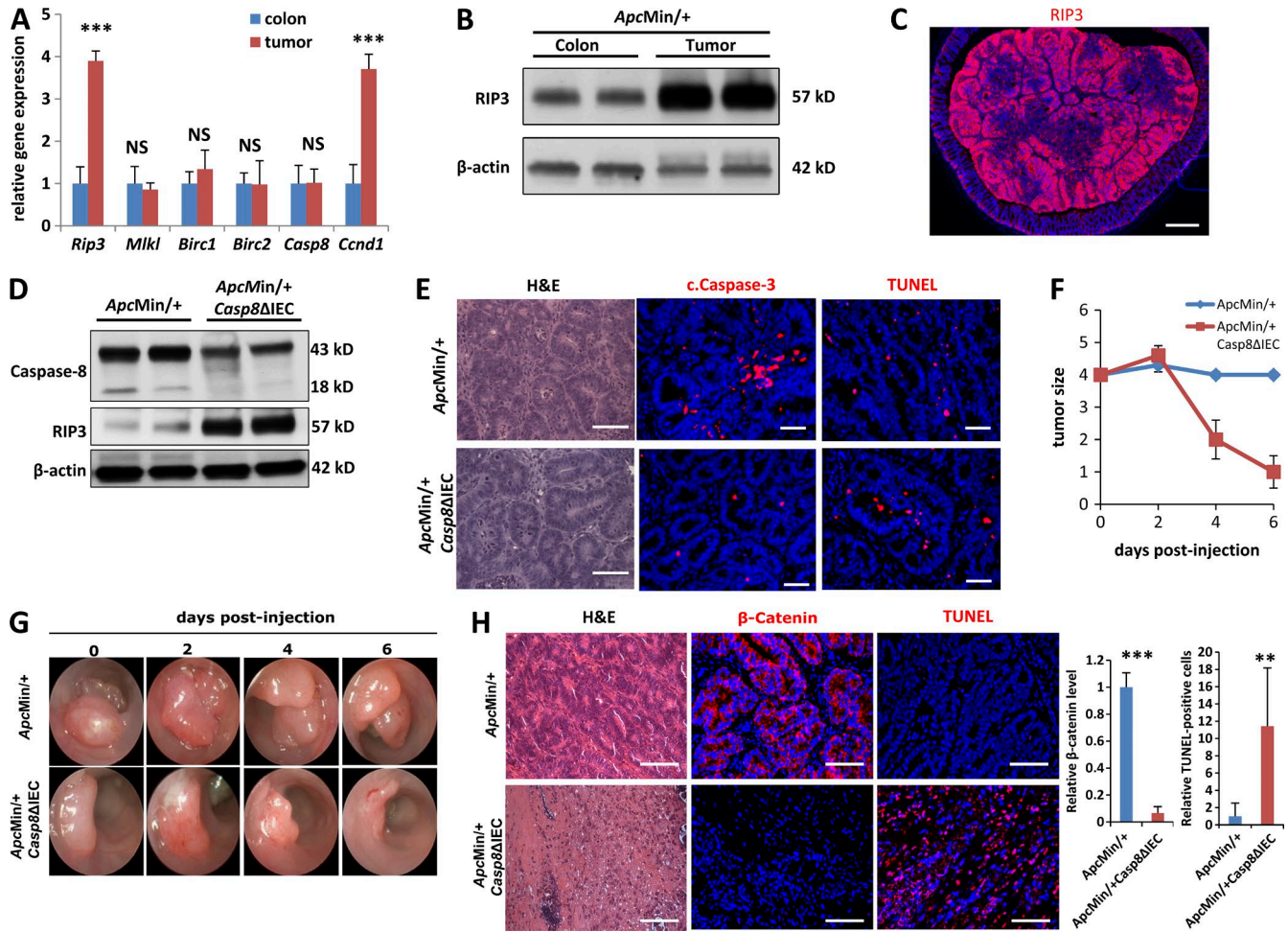


Figure 2. Loss of caspase-8 sensitizes mouse colon tumors to SMAC mimetic. (A–C) Tumors and tumor-adjacent colon tissues were collected from 14-wk-old *ApcMin/+* mice. (A) Quantitative RT-PCR analysis of gene expression indicated on the x axis. Gene expression was normalized to *Hprt*. Group sizes: $n = 11$; NS, $P > 0.05$; ***, $P < 0.001$. (B) Immunoblots of tissue extracts. (C) Immunostaining of colon cross sections with a RIP3 antibody. (D) Immunoblots of tumor tissue extracts from *ApcMin/+* mice and *ApcMin/+ Casp8ΔIEC* mice. (B and D) β -Actin served as a loading control. (E) Tumor cross-sections from indicated mice were subjected to staining of H&E (left), cleaved caspase-3 (middle), and TUNEL (right). (F–H) *ApcMin/+* mice and *ApcMin/+ Casp8ΔIEC* mice bearing size 4 tumors were intratumorally injected with LCL161 (100 μ g/tumor). (F and G) The size of tumors was scored by colonoscopy every second day for 6 d. Group size: $n = 5$. (G) Representative colonoscopy imaging of tumors. (H) 2 d after injection of LCL161, tumors were collected for staining of H&E, mouse β -catenin (quantification is shown on the right), and TUNEL (quantification is shown on the right). **, $P < 0.01$; ***, $P < 0.001$. Results from at least three biological replicates are presented unless otherwise specified. Data derived from two independent animal experiments are shown (F–H). Bars: (C) 500 μ m; (E and H) 75 μ m. Error bars indicate \pm SD.

A). Histological analysis revealed a massive loss of tumor cells stained with β -catenin and a great reduction in proliferating cells stained with Ki67 only in C8KO-luc-D6–derived tumors from SMAC mimetic–treated mice (Fig. 3, G and H; and Fig. S3, B, C, and E). The majority of cell death events were negative for cleaved caspase-3, indicating that these cells died of necroptosis rather than apoptosis (Fig. 3 I and Fig. S3 D). Moreover, tumor cells with low rather than absent caspase-8 were also significantly susceptible to SMAC mimetic–induced necroptosis in vivo (Fig. S3, I and J). Collectively, these data demonstrate that SMAC mimetic alone is efficient to treat human tumors deficient in caspase-8 in vivo.

In conclusion, our data provided solid evidence that SMAC mimetic alone is efficient to treat colorectal tumors with caspase-8 deficiency in both a hereditary and a xenograft mouse model. Of note, multiple lines of evidence have revealed that caspase-8 expression is frequently absent in many types of human cancers via multiple mechanisms. In particular, complete inactivation of caspase-8 has been identified in human neuroblastomas through DNA methylation and gene deletion (Hopkins–Donaldson et al., 2000; Teitz et al., 2000; Pingoud–Meier et al., 2003). Caspase-8 deficiency is frequently found in human CRCs refractory to current therapeutic approaches via evasion of apoptosis. Importantly,

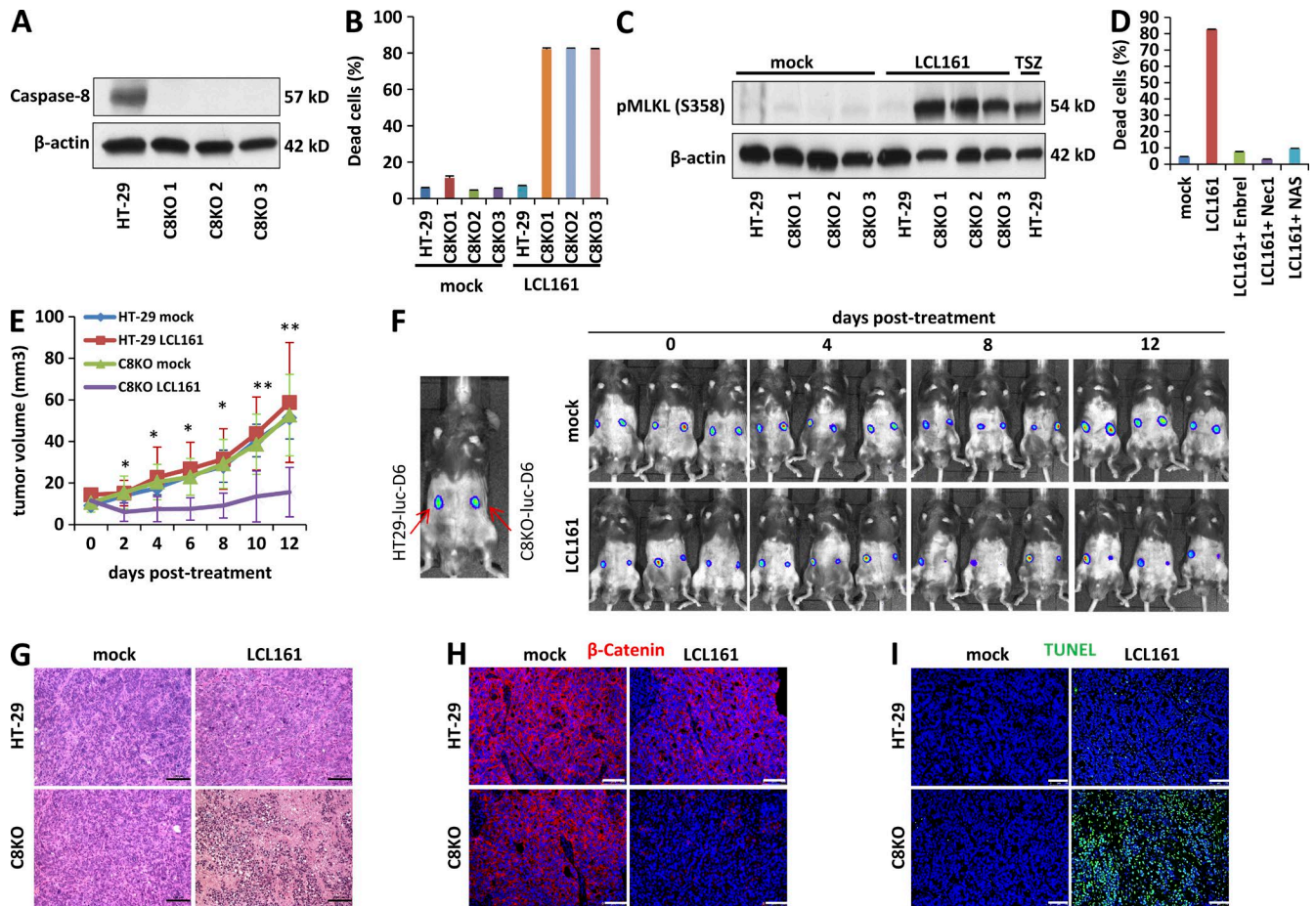


Figure 3. *Caspase-8* deficiency renders human CRC cells and xenograft human tumors hypersensitive to SMAC mimetic-induced necroptosis. (A–D) In vitro effect of SMAC mimetic on HT-29 cells and *caspase-8*-knockout C8KO cells generated with CRISPR/Cas9 plasmids. (B and D) Error bars indicate +SD. (A) Validation of *caspase-8*-knockout efficiency with immunoblots. β -Actin served as a loading control. (B) Cell death assay with propidium iodide staining followed by flow cytometry analysis. (C) Immunoblot of phospho-MLKL (S358) in the indicated cells treated with DMSO or 100 nM LCL161 for 18 h. An HT-29 cell treated with 20 ng/ml TNF (T) + 100 nM SMAC mimetic (S) + 20 μ M zVAD (Z) served as a positive control. (D) Cell death assay with propidium iodide staining followed by flow cytometry analysis. Enbrel, Nec1, and NAS were added 30 min before LCL161. (E–I) Mice with established subcutaneous HT-29/HT-29-luc-D6 tumors (left side tumors) and C8KO/C8KO-luc-D6 tumors (right side tumors) were treated with PBS (mock) or 50 mg/kg LCL161 (oral) every second day. Tumor growth was monitored for 12 d by caliper (E) and in vivo imaging (F) measurements. Error bars indicate \pm SD; *, $P < 0.05$; **, $P < 0.01$. (G–I) Tumors from mice treated with LCL161 for 3 d were stained with H&E (bars, 100 μ m), human β -catenin (bars, 100 μ m), or TUNEL (bars, 75 μ m). Results from at least three biological replicates are presented unless otherwise specified. Data are derived from two independent animal experiments (E–I).

a functional study has indicated that *caspase-8* mutations found in human CRC can markedly decrease apoptosis activity, and these mutants showed a dominant-negative inhibition of death receptor-induced apoptosis (Kim et al., 2003). These studies have clearly demonstrated the relevance of *caspase-8* deficiency in human cancer, including CRC. Our findings therefore represent an attractive strategy for overcoming apoptosis resistance by inducing necroptosis. Given that several SMAC mimetics are being evaluated in clinical trials in cancer patients, our study suggests that it may be worthwhile to selectively evaluate the efficacy of SMAC mimetics treatment in CRC patients with *caspase-8* deficiency for the development of a more effective personalized therapy.

MATERIALS AND METHODS

Mice

Mice carrying a *loxP*-flanked *caspase-8* allele (*Casp8^{fl}*) and villin-*Cre* mice were described earlier (Madison et al., 2002; El Marjou et al., 2004; Beisner et al., 2005). *Casp8 Δ IEC* mice, *Casp8 Δ IEC* \times *Tnfr1*^{-/-}, and *Casp8 Δ IEC* \times *Rip3*^{-/-} mice were previously used in our studies (Günther et al., 2011, 2015). For SMAC mimetic treatment, the LCL161 orally bioavailable chemical compound (gift of D. Porter, Novartis Institutes for BioMedical Research, Boston, MA) was dissolved in PBS with 0.73% of 0.1 N HCl and was orally administered to mice (50 mg/kg) except for intratumoral injection. Experiments were performed under protocols approved by

the Institutional Animal Care and Use Committee of the University of Erlangen.

Cell culture

All human CRC cell lines were cultured in DMEM (Invitrogen) supplemented with 10% heat-inactivated FCS (Invitrogen) and 1% penicillin/streptomycin (Invitrogen) and maintained at 37°C and 5% CO₂. HT-29, HCT116, SW480, SW620, Caco2, and DLD-1 cancer cell lines were from ATCC. The luciferase expressing cell line HT-29-luc-D6 was from PerkinElmer. All cell cultures were free of mycoplasma contamination.

Cell death assay

For the induction of necroptosis, either 100 nM LCL161 alone or a combination of 100 nM LCL161, 20 ng/ml TNF (R&D Systems), and 20 μM zVAD (Bachem) was used as indicated. For the inhibition of necroptosis, 5 μg/ml Enbrel (Pfizer), 10 μM Nec1 (Bachem), and 1 μM NAS (EMD Millipore) were added 30 min before LCL161. Cells were stained with propidium iodide and analyzed with flow cytometry (LSR Fortessa II; BD). Alternatively, cell culture supernatant was collected for LDH assay.

Stable cell line generation

Caspase-8-knockout cell lines were generated from human adenocarcinoma cell line HT-29 (ATCC) and a luciferase-expressing cell line HT-29-luc-D6 (Caliper) using CRISPR/Cas9 KO Plasmid (Santa Cruz Biotechnology, Inc.) according to the protocol of the supplier. For generation of single-cell colonies, GFP-positive cells were sorted into 96-well plates (one cell/well) by flow cytometry (FACSARIA II; BD).

For the creation of stable cell lines with lower caspase-8 expression, HT-29 cells were transfected with retroviral plasmids of negative control shRNA or caspase-8 shRNA (TG305635; OriGene). The transfected cells were cultured in growth medium containing 1 μg/ml puromycin for selection.

Immunoblotting

Proteins were isolated from cells or tissues using Mammalian Protein Extraction reagent (Thermo Fisher Scientific) supplemented with protease inhibitors (Complete Mini Protease Inhibitor Cocktail; Roche) and phosphatase inhibitors (PhosphoStop Phosphatase Inhibitor Cocktail; Roche). Proteins were separated using a MiniProtean-TGX gel (4–15% polyacrylamide; Bio-Rad Laboratories) and transferred from the gel to a nitrocellulose membrane (Whatman). Membranes were probed with the following primary antibodies: anti-mouse RIP3 (ADI-905-242-100; Enzo Life Sciences), anti-human RIP3 (13526; Cell Signaling Technology), anti-mouse cleaved caspase-8 (8592; Cell Signaling Technology), anti-caspase-8 (4790; Cell Signaling Technology), anti-human phospho-MLKL (S358, ab187091; Abcam), and HRP-linked β-actin (ab49900; Abcam). HRP-linked anti-rabbit IgG (7074; Cell Signaling Technology) was used as a secondary antibody.

Real-time quantitative RT-PCR

Total RNA was extracted from cells and tissues using the peqGOLD MicroSpin Total RNA kit and peqGOLD Total RNA kit (Peqlab), respectively. cDNA was synthesized using the SCRIPT cDNA Synthesis kit from Jena Bioscience and analyzed by real-time PCR using specific QuantiTect Primer assays (QIAGEN). Experimental values were normalized to levels of the housekeeping gene hypoxanthine guanine phosphoribosyl transferase (HPRT).

xCELLigence

The cell index was monitored with an xCELLigence Real-Time Cell Analyzer (RTCA) instrument with E-Plate 16 (Roche) according to the manufacturer's protocol. The cell index was normalized with the RTCA software 1.2.1 (Roche).

Tumor models

For HT-29 xenograft model, 2×10^6 cancer cells were injected subcutaneously in 100 μl PBS into the flanks of 6–10-wk-old *Rag1*^{-/-} mice as indicated. One week later, mice bearing palpable tumors were orally administered 50 mg/kg vehicle or LCL161 every second day. Tumors were measured at serial time points after LCL161 treatment using a digital caliper and the tumor volume was calculated using $V = (\text{length} \times \text{width} \times \text{height})/2$.

For *ApcMin*/+ model, 14-wk-old mice bearing colon tumors were orally administered a single dose of 50 mg/kg LCL161, and tumors were collected 24 h later. For intratumoral injection, mice bearing colon tumors of size 4 were used. A single dose of LCL161 (100 μg/tumor) was injected directly into the tumor using colonoscopy, and the tumor was scored with colonoscopy every second day as previously described (Becker et al., 2005; Neurath et al., 2010).

For the AOM/DSS model, we followed a previously described protocol to induce colon tumors in WT B6 mice (Neufert et al., 2007).

In vivo bioluminescent assay

Mice bearing HT-29-luc-D6 tumor and *caspase-8*-knockout HT-29-luc-D6 (HT-29-luc-D6-C8KO) tumors were injected i.p. with 10 μl/g body weight of Luciferin (Promega) in 100 μl PBS and imaged with IVIS Lumina (PerkinElmer).

Histology and immunofluorescence

Histopathological analyses were performed on formalin-fixed paraffin-embedded tissue after Mayer's H&E staining. Immunofluorescence of tissue sections was performed using the TSA Cy3 system as recommended by the manufacturer (PerkinElmer). Anti-mouse RIP3 (ADI-905-242-100; Enzo Life Sciences), anti-mouse β-catenin (8480; Cell Signaling Technology), and anti-human β-catenin (4176; Cell Signaling Technology) antibodies were used for immunofluorescence staining. Nuclei were counterstained with Hoechst 3342 (Invitrogen). Cell death was determined by TUNEL (terminal deoxynucleotidyl transferase dUTP nick end label-

ing) analysis using the in situ cell death detection kit (Roche). Images were obtained using the microscope Leica DMI 4000B (Leica Microsystems).

Statistics

A two-tailed Student's *t* test was applied to calculate statistical significance of the difference in sample means (*, $P \leq 0.05$; **, $P \leq 0.01$; ***, $P \leq 0.001$; N.S., not significant; SD).

Online supplemental material

Fig. S1 shows additional data supporting that SMAC mimetic induces necroptosis in mouse IECs and tumor cells. Fig. S2 shows additional data supporting that SMAC mimetic induces necroptosis in human CRC cell lines in vitro. Fig. S3 shows additional data supporting that SMAC mimetic induces necroptosis in a xenograft model of human CRC.

ACKNOWLEDGMENTS

We thank D. Porter for providing LCL161 and S. Wallmüller, K. Urbanová, H. Dörner, and G. Förtsch for excellent technical assistance.

The research leading to these results has received funding from Deutsche Forschungsgemeinschaft project BE3686/2, research unit FOR2438, SFB1181, SFB796, SPP1656, and clinical research unit KF0257. Further support was given by the Interdisciplinary Center for Clinical Research (IZKF) of the University of Erlangen-Nuremberg and the European Community's Seventh Framework Program (acronym BTCure).

The authors declare no competing financial interests.

Author contributions: G.-W. He and C. Becker designed the research. G.-W. He, C. Becker, M.F. Neurath, and M. Stürzl analyzed the data and wrote the paper. G.-W. He, C. Günther, V. Thonn, Y.-Q. Yu, E. Martini, and B. Buchen performed the experiments.

Submitted: 29 March 2016

Revised: 12 January 2017

Accepted: 23 March 2017

REFERENCES

- Becker, C., M.C. Fantini, S. Wirtz, A. Nikolaev, R. Kiesslich, H.A. Lehr, P.R. Galle, and M.F. Neurath. 2005. In vivo imaging of colitis and colon cancer development in mice using high resolution chromoendoscopy. *Gut*. 54:950–954. <http://dx.doi.org/10.1136/gut.2004.061283>
- Beisner, D.R., I.L. Ch'en, R.V. Kolla, A. Hoffmann, and S.M. Hedrick. 2005. Cutting edge: Innate immunity conferred by B cells is regulated by caspase-8. *J. Immunol.* 175:3469–3473. <http://dx.doi.org/10.4049/jimmunol.175.6.3469>
- Cancer Genome Atlas Network. 2012. Comprehensive molecular characterization of human colon and rectal cancer. *Nature*. 487:330–337. <http://dx.doi.org/10.1038/nature11252>
- Degterev, A., M. Boyce, and J. Yuan. 2003. A decade of caspases. *Oncogene*. 22:8543–8567. <http://dx.doi.org/10.1038/sj.onc.1207107>
- El Marjou, F., K.P. Janssen, B.H. Chang, M. Li, V. Hindie, L. Chan, D. Louvard, P. Chambon, D. Metzger, and S. Robine. 2004. Tissue-specific and inducible Cre-mediated recombination in the gut epithelium. *Genesis*. 39:186–193. <http://dx.doi.org/10.1002/gene.20042>
- Feoktistova, M., P. Geserick, B. Kellert, D.P. Dimitrova, C. Langlais, M. Hupe, K. Cain, M. MacFarlane, G. Häcker, and M. Leverkus. 2011. cIAPs block Ripoptosome formation, a RIP1/caspase-8 containing intracellular cell death complex differentially regulated by cFLIP isoforms. *Mol. Cell*. 43:449–463. <http://dx.doi.org/10.1016/j.molcel.2011.06.011>
- Fulda, S. 2009. Caspase-8 in cancer biology and therapy. *Cancer Lett.* 281:128–133. <http://dx.doi.org/10.1016/j.canlet.2008.11.023>
- Fulda, S., and D. Vucic. 2012. Targeting IAP proteins for therapeutic intervention in cancer. *Nat. Rev. Drug Discov.* 11:109–124. <http://dx.doi.org/10.1038/nrd3627>
- Günther, C., E. Martini, N. Wittkopf, K. Amann, B. Weigmann, H. Neumann, M.J. Waldner, S.M. Hedrick, S. Tenzer, M.F. Neurath, and C. Becker. 2011. Caspase-8 regulates TNF- α -induced epithelial necroptosis and terminal ileitis. *Nature*. 477:335–339. <http://dx.doi.org/10.1038/nature10400>
- Günther, C., B. Buchen, G.W. He, M. Hornef, N. Torow, H. Neumann, N. Wittkopf, E. Martini, M. Basic, A. Bleich, et al. 2015. Caspase-8 controls the gut response to microbial challenges by Tnf- α -dependent and independent pathways. *Gut*. 64:601–610. <http://dx.doi.org/10.1136/gutjnl-2014-307226>
- Hanahan, D., and R.A. Weinberg. 2011. Hallmarks of cancer: The next generation. *Cell*. 144:646–674. <http://dx.doi.org/10.1016/j.cell.2011.02.013>
- He, S., L. Wang, L. Miao, T. Wang, F. Du, L. Zhao, and X. Wang. 2009. Receptor interacting protein kinase-3 determines cellular necrotic response to TNF- α . *Cell*. 137:1100–1111. <http://dx.doi.org/10.1016/j.cell.2009.05.021>
- Hopkins-Donaldson, S., J.L. Bodmer, K.B. Bouloud, C.B. Brognara, J. Tschopp, and N. Gross. 2000. Loss of caspase-8 expression in highly malignant human neuroblastoma cells correlates with resistance to tumor necrosis factor-related apoptosis-inducing ligand-induced apoptosis. *Cancer Res.* 60:4315–4319.
- Kaiser, W.J., J.W. Upton, A.B. Long, D. Livingston-Rosanoff, L.P. Daley-Bauer, R. Hakem, T. Caspary, and E.S. Mocarski. 2011. RIP3 mediates the embryonic lethality of caspase-8-deficient mice. *Nature*. 471:368–372. <http://dx.doi.org/10.1038/nature09857>
- Kim, H.S., J.W. Lee, Y.H. Soung, W.S. Park, S.Y. Kim, J.H. Lee, J.Y. Park, Y.G. Cho, C.J. Kim, S.W. Jeong, et al. 2003. Inactivating mutations of caspase-8 gene in colorectal carcinomas. *Gastroenterology*. 125:708–715. [http://dx.doi.org/10.1016/S0016-5085\(03\)01059-X](http://dx.doi.org/10.1016/S0016-5085(03)01059-X)
- Li, C., A.M. Egloff, M. Sen, J.R. Grandis, and D.E. Johnson. 2014. Caspase-8 mutations in head and neck cancer confer resistance to death receptor-mediated apoptosis and enhance migration, invasion, and tumor growth. *Mol. Oncol.* 8:1220–1230. <http://dx.doi.org/10.1016/j.molonc.2014.03.018>
- Madison, B.B., L. Dunbar, X.T. Qiao, K. Braunstein, E. Braunstein, and D.L. Gumucio. 2002. Cis elements of the villin gene control expression in restricted domains of the vertical (crypt) and horizontal (duodenum, cecum) axes of the intestine. *J. Biol. Chem.* 277:33275–33283. <http://dx.doi.org/10.1074/jbc.M204935200>
- Neufert, C., C. Becker, and M.F. Neurath. 2007. An inducible mouse model of colon carcinogenesis for the analysis of sporadic and inflammation-driven tumor progression. *Nat. Protoc.* 2:1998–2004. <http://dx.doi.org/10.1038/nprot.2007.279>
- Neurath, M.F., N. Wittkopf, A. Wlodarski, M. Waldner, C. Neufert, S. Wirtz, C. Günther, and C. Becker. 2010. Assessment of tumor development and wound healing using endoscopic techniques in mice. *Gastroenterology*. 139:1837–1843.e1. <http://dx.doi.org/10.1053/j.gastro.2010.10.007>
- Oberst, A., C.P. Dillon, R. Weinlich, L.L. McCormick, P. Fitzgerald, C. Pop, R. Hakem, G.S. Salvesen, and D.R. Green. 2011. Catalytic activity of the caspase-8-FLIP₁ complex inhibits RIPK3-dependent necrosis. *Nature*. 471:363–367. <http://dx.doi.org/10.1038/nature09852>
- Petersen, S.L., L. Wang, A. Yalcin-Chin, L. Li, M. Peyton, J. Minna, P. Harran, and X. Wang. 2007. Autocrine TNF α signaling renders human cancer cells susceptible to Smac-mimetic-induced apoptosis. *Cancer Cell*. 12:445–456. <http://dx.doi.org/10.1016/j.ccr.2007.08.029>
- Pingoud-Meier, C., D. Lang, A.J. Jans, L.B. Rorke, P.C. Phillips, T. Shalaby, and M.A. Grotzer. 2003. Loss of caspase-8 protein expression correlates with unfavorable survival outcome in childhood medulloblastoma. *Clin. Cancer Res.* 9:6401–6409.

- Teitz, T., T. Wei, M.B. Valentine, E.F. Vanin, J. Grenet, V.A. Valentine, F.G. Behm, A.T. Look, J.M. Lahti, and V.J. Kidd. 2000. Caspase 8 is deleted or silenced preferentially in childhood neuroblastomas with amplification of MYCN. *Nat. Med.* 6:529–535. <http://dx.doi.org/10.1038/75007>
- Vandenabeele, P., L. Galluzzi, T. Vanden Berghe, and G. Kroemer. 2010. Molecular mechanisms of necroptosis: An ordered cellular explosion. *Nat. Rev. Mol. Cell Biol.* 11:700–714. <http://dx.doi.org/10.1038/nrm2970>
- Wittkopf, N., C. Günther, E. Martini, G. He, K. Amann, Y.W. He, M. Schuchmann, M.F. Neurath, and C. Becker. 2013. Cellular FLICE-like inhibitory protein secures intestinal epithelial cell survival and immune homeostasis by regulating caspase-8. *Gastroenterology.* 145:1369–1379. <http://dx.doi.org/10.1053/j.gastro.2013.08.059>